RSC Advances

PAPER

View Article Online
View Journal | View Issue

Cite this: *RSC Adv.*, 2021, **11**, 27607

Low temperature NH_3-SCR performance and mechanism of Mn and Fe supported $CeCO_3F$-monazite catalysts†

Na Li,[ab] Shenghan Zhang,[*a] Zedong Cheng[b] and Wenfei Wu[b]

The group has shown that Baiyun Ebo rare earth concentrate has excellent performance in NH_3-SCR denitrification when used as a carrier, where rare earth elements are mainly present in cerium fluorocarbon ore ($CeCO_3F$) and monazite ($CePO_4$) mineral phases. In this paper, a new low-temperature NH_3-SCR catalyst of Mn–Fe/$CeCO_3F$-monazite was prepared by an impregnation method, using synthetic $CeCO_3F$ and purified monazite as carriers. By exploring its denitrification performance and mechanistic analysis, it provides theoretical guidance for the use of rare earth concentrates as low-temperature NH_3-SCR catalysts. Our previous studies have determined the optimum loading of Fe, so this paper needs to be investigated for the optimum doping ratio of the active substance Mn. The results of the activity tests, XRD and BET have determined that the best denitrification rate and catalytic performance was achieved at a ratio of Mn : Ce of 1 : 5. The denitrification activity of the different catalysts was investigated by loading Fe, Mn and Fe and Mn together. The results obtained by means of experimental analyses such as XRD, SEM, BET and activity tests showed that the composite catalyst loaded with Fe and Mn at the same time, had the highest activity and its denitrification rate could reach 94.8% at 250 °C. This is mainly attributed to the fact that the interaction of Fe, Mn can promote the dispersion of each other on the carrier surface, which greatly improves the specific surface area of the catalyst. The introduction of Fe and Mn increases the acidic sites and the amount of acid on the catalyst surface, which results in the formation of a large number of oxygen vacancies and the presence of more oxygen species on the catalyst surface, which facilitate the migration of oxygen. The new catalyst was investigated by Fourier transform infrared (FTIR) spectroscopy to characterise the adsorption and transformation behaviour of the reactive species on the surface of the catalyst, and to investigate the reaction mechanism. The results showed that the entire reaction process followed the L–H mechanism, with the gaseous NO adsorption and activation on the catalyst surface generating bidentate nitrate, bridging nitrate species and NH_3/NH_4^+ species as the main intermediate species involved in the reaction, both of which underwent redox reactions on the catalyst surface to produce N_2 and H_2O. The above results indicated that the $CeCO_3F$-monazite carrier has excellent performance, and provided a theoretical basis for the high-value utilization of rare earth concentrates.

Received 15th July 2021
Accepted 3rd August 2021

DOI: 10.1039/d1ra05435j

rsc.li/rsc-advances

1. Introduction

The production of NO_x from coal, diesel and gasoline causes a number of environmental problems such as photochemical smog and ozone depletion.[1] Therefore NO_x reduction and removal is imperative. The commercial V_2O_5-WO_3(MoO_3)/TiO_2 catalyst for the selective catalytic reduction (SCR) of NH_3 from NO_x is a widely used technology for the removal of NO_x from coal combustion.[2] However, problems such as the toxicity of V_2O_5 and the narrow activity temperature window (320–400 °C) remain.[3,4] Therefore, we need to develop efficient and environmentally friendly catalysts for low temperature NH_3-SCR.

In recent years, rare earth element catalysts have been widely studied in the field of NH_3-SCR due to their abundant storage capacity as well as their stable properties, which not only have good catalytic activity but also good tolerability. Wang *et al.*[5] used a hydrothermal method to load different rare earth oxides (La, Ce, Pr, Nd) onto activated semi-coke (ASC) to prepare low temperature (150–300 °C) selective catalytic reduction (SCR) catalysts for NH_3 to NO. The results showed that the best performance of the CeO_2-loaded catalysts was due to the doping of rare earth elements which effectively promoted the increase of oxygen vacancy concentration. The high concentration of

[a]North China Electric Power University, School of Environmental Science and Engineering, Baoding 071000, Hebei, China. E-mail: shenghan_zhang@126.com
[b]Inner Mongolia University of Science & Technology, School of Energy and Environment, Baotou 014010, Inner Mongolia, China

† Electronic supplementary information (ESI) available. See DOI: 10.1039/d1ra05435j

oxygen vacancies not only facilitated the formation of lattice oxygen, but also the adsorption of O_2 and the further oxidation of NO. The lattice oxygen initially oxidised the NO to NO_2, which facilitated the subsequent reduction reaction to proceed rapidly. Jie Fan[6] *et al.* evaluated the effect of cerium or lanthanum on the hydrothermal stability of copper-SAPO-3 catalysts. The results showed that the nitrogen oxide conversion of aged cerium or lanthanum modified Cu-SAPO-34 remained above 93%. This is because the introduction of cerium or lanthanum effectively slowed down the dealumination process, and inhibited the aggregation of copper species on Cu-SAPO-34 during hydrothermal ageing, further maintaining a relatively large specific surface area and uniform pore size distribution. At the same time, the redox properties of Cu-SAPO-34 were enhanced and the surface acidic sites were stabilised, further facilitating the adsorption and activation of the reactants.

Baiyun Ebo rare earth minerals are rich in rare earth elements and have been used to good effect in the preparation of NH_3-SCR catalysts. There has been some progress in the preparation of denitrification catalysts directly from minerals (rare earth concentrates, rare earth tailings), which contain not only many rare earth elements, but also some transition metals, which can significantly improve the denitrification efficiency. Meng Zhaolei[7] *et al.* used Fe_2O_3 loaded on Baiyun Ebo rare earth concentrate by impregnation method, and the denitrification rate could reach more than 80% at 350 °C. The catalyst surface became rough and porous, which increased the specific surface area; and most of the Fe_2O_3 was embedded on the rare earth concentrate in a highly dispersed or amorphous form, which formed a small portion of FeCeO composite oxide. Zhang[8] *et al.* prepared catalysts by using roasted weak acid-weak base leaching method for the denitrification of rare earth concentrates. The denitrification rate was up to 92.8% at 400 °C. The results showed that the Ce_7O_{12} content in the active fraction increased and was more uniformly distributed. The specific surface area increased and the exposure of active sites increased. Wang Jian[9] *et al.* used different microwave roasting temperatures to treat the tailings, resulting in a denitrification rate of up to 96.1% at 400 °C. This has guiding significance for the efficient use of rare earth tailings. However, the current research on catalysts prepared using rare-earth concentrates and rare-earth tailings has focused on medium and high temperatures, and there has been no relevant research on their low temperature NH_3-SCR performance.

From the process mineralogy of Baiyun Ebo rare earth concentrates,[10] it can be obtained that the rare earth minerals are mainly dominated by Ce elements. Ce based catalysts have excellent low temperature catalytic properties, and many researchers have used CeO_2 as a carrier to improve the performance of NH_3-SCR. Zhang Runduo[11] *et al.* prepared $LaMnO_3$, $LaMnO_3/TiO_2$ and $LaMnO_3/CeO_2$ catalysts to investigate the effect of the carrier on the catalytic performance of NH_3-SCR, and the results showed that the best low-temperature catalytic performance was achieved with CeO_2 as the carrier. The main reason is that at temperatures less than 200 °C, the interaction between $LaMnO_3$ and CeO_2 facilitates the movement of lattice oxygen, which can promote partial oxidation of NO to NO_2, allowing the NO reduction reaction to proceed according to the fast NH_3-SCR reaction. Yao Xiaojiang[12] prepared a series of MnO_x/CeO_2 catalysts by adjusting the solvents (deionised water, anhydrous ethanol, acetic acid, oxalic acid solution). The MnO_x/CeO_2 catalysts prepared with oxalic acid solution as the solvent showed over 80% NO conversion in the range of 100–250 °C and good low temperature sulphur and water resistance. The rare earth elements in rare earth concentrates are mainly found in cerium fluorocarbon and monazite, with Ce elements accounting for more than 38% of the total. As purified cerium fluoride ore is currently unavailable, I[13] have used a hydrothermal method to synthesise cerium fluoride ore, which is highly compatible with the mineral phase of cerium fluoride ore in the concentrate. Natural monazite ore can be obtained from the Baiyun Ebo. So this experiment will use the synthesized fluorocerium cerium ore and purified monazite ore together as a carrier, loaded with Mn and Fe active substances, and provide theoretical guidance significance for the use of rare earth minerals of dolomite as a denitrification catalyst carrier by exploring its excellent performance and mechanism as a low-temperature denitrification catalyst carrier.

2. Experimental methods

2.1. Materials and methods

In this paper, $CeCO_3F$ was synthesised by hydrothermal method using cerium nitrate as raw material, mixed with sodium bicarbonate and sodium fluoride. The synthesized $CeCO_3F$ was mixed with monazite ore purified from dolomite concentrate as a carrier and loaded with Mn and Fe in a certain ratio. The surface properties and denitrification activity were tested to determine the best catalyst. The chemical reagents used in the experiments were: $Ce(NO_3)_3 \cdot 6H_2O$ (mass fraction), analytical purity, Tianjin Comio Chemical Reagent Co. $NaHCO_3$, analytical purity, Tianjin Windship Chemical Reagent Technology Co. NaF, analytical purity, Tianjin Windship Chemical Reagent Technology Co. Monazite ore is monazite ore obtained from the purification of Baiyun Ebo concentrate.

2.2. Preparation of the catalyst

The hydrothermal method was used to synthesize $CeCO_3F$. A certain amount of $Ce(NO_3)_3 \cdot 6H_2O$ was placed in 100 mL of PTFE liner at room temperature, and a certain amount of NaF and $NaHCO_3$ was dissolved in 80 mL of distilled water. The mixed solution was poured into the PTFE liner and put into an autoclave at 120 °C under atmospheric pressure and stirred and heated for 2 h for hydrothermal reaction. After cooling, the mixture is filtered and dried at 110 °C to obtain synthetic cerium fluorocarbon ore. The synthetic cerium fluorocarbon ore and a certain amount of monazite ore were then mixed and impregnated at room temperature for 24 h, filtered and dried to obtain $CeCO_3F$-monazite carrier. It was divided into several portions and loaded with Mn according to the molar ratio of Ce in the carrier, and 50% $Mn(NO_3)_2$ solution was added dropwise to the carrier in the ratio of Ce : Mn = 2 : 1, Ce : Mn = 5 : 1, Ce : Mn = 8 : 1, respectively. It was transferred to 100 mL of distilled water and macerated for

24 h. The solution was filtered and dried at 110 °C. Finally, the sample was microwave roasted at 500 °C for 5 min to obtain the catalyst loaded with Mn. In the same way, Fe_2O_3 was added to the carrier in the ratio of Ce : Fe = 5 : 1, then the solution was impregnated for 24 h, filtered and dried, and roasted at 500 °C for 5 minutes to obtain catalysts loaded with Fe. The catalyst was tested for catalytic performance and the optimum Mn loading and Fe loading were selected, which will be loaded onto the carrier in the ratio of Mn : Fe = 1 : 1.

2.3. Testing of catalytic performance

The experiments were carried out in a reaction apparatus with quartz tubes for testing the activity of the catalyst NH_3-SCR. The reaction apparatus consists of a gas mixing tank – flow meter, standpipe furnace, quartz tube, Fourier infrared spectroscopy flue gas analyser and computer data acquisition system. The standpipe furnace was heated by a silicon-molybdenum rod model 1800 with a rated temperature of 1600 °C and an internal diameter of 20 mm and a length of 1.2 m from Nanjing Boynton Instrument Technology Co. The Fourier infrared spectroscopy (FTIR) flue gas analyser and data acquisition system were manufactured in Finland, and the model number was GASMET-DX4000. The simulated gas components were as follows: NH_3 500 ppm, NO 500 ppm, O_2 at a volume fraction of 3% of the total, N_2 as the equilibrium gas, a total gas flow of 100 mL min^{-1}, an air velocity of approximately 8000 h^{-1} g^{-1} and a catalyst dosage of 0.6 g for each test.

Firstly, the test equipment and controls such as the gas cylinder valve are opened and a constant gas flow rate in the empty tube is carried out so that the gas flow in the gas path is constant and the gas content detected by the flue gas analyser is stable. Then the quartz wool and catalyst are placed in the quartz tube and warmed up to test the denitrification activity of the catalyst in the temperature range of 100 °C to 400 °C. The denitration data is recorded at 50 °C intervals and the constant temperature time at each temperature point is 15 min. The content of the gas measured by the flue gas analyser during this time is the NO_x content of the treated virtual flue gas.

The formula for calculating the denitration rate of the catalyst treated by the activity test is:

$$\eta = \frac{(NO)_{in} - (NO)_{out}}{(NO)_{out}} \times 100\%$$

η is the NO removal rate; (NO)in is the percentage of NO detected after smoothing the inlet of the flue gas simulation system; (NO)out is the percentage of NO detected by the flue gas analyser at the outlet test of the flue gas simulation system.

2.4. Characterisation of the catalysts

XRD diffractometer type D8 ADVANCE, BRUKER, Germany; angle of, range 10° to 80°. Observation of the surface structure and morphology of the catalyst using a field emission scanning electron microscope type 500 AMCS, Carl Zeiss, Germany. Simulated flue gas denitrification unit (including flowmeter, heating furnace, Beijing Pioid Electronic Technology Co., Ltd; Laoying 3022 comprehensive flue gas analyser, Laoshan Institute of Applied Technology, Qingdao). Programmed temperature rise desorption (TPD) and programmed temperature rise reduction (TPR) were carried out on a chemisorption instrument (from Beijing Peod Electronic Technology Co., Ltd.) with a thermal conductivity detector (TCD). A 0.2 g sample of catalyst was purged under N2 atmosphere for 10 min prior to the experiment and dehydrated at a constant temperature of 200 °C for 30 min, followed by NH_3 adsorption at 100 °C for one hour. Finally the catalyst was ramped up from 50 °C to 600 °C at a rate of 10 °C min^{-1}. For H_2-TPR, the catalyst samples were ramped up from 50 °C to 800 °C at a rate of 10 °C min^{-1}.

3. Results and discussion

3.1. Experiments on the optimum Mn loading

3.1.1 Testing of the catalytic performance. Our previous pre-experimental results showed that, the best catalytic performance was obtained by loading Fe_2O_3 onto $CeCO_3F$ plus monazite at a ratio of 5 : 1 Ce : Fe. Therefore, in this paper, only the catalyst loaded with Fe alone was tested for denitrification

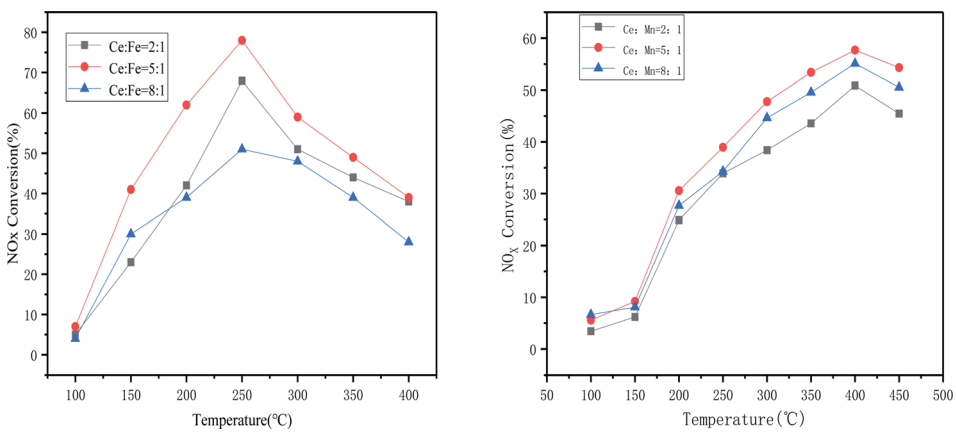

Fig. 1 NH_3-SCR activity of $CeCO_3F$-monazite loaded with different proportions of Mn and Fe (reaction conditions: 500 ppm NO, 500 ppm NH_3, 3% O_2, N_2 as equilibrium gas).

performance. The results showed that the catalyst loaded with Fe alone gave a NO_x conversion of 79% at 250 °C. In order to investigate the optimum loading of synthetic $CeCO_3F$ plus monazite loaded Mn, the denitrification activity was tested and the results are shown in Fig. 1. It can be seen from the figure that before 150 °C, the catalyst activity was relatively low for different percentages of Mn loadings, stabilising within 10%. After 150 °C, the catalytic performance of the catalysts improved significantly due to the interaction between Mn and Ce, which showed good catalytic activity. The denitrification rate of the three catalysts began to rise rapidly, reaching the highest rate at 400 °C, with the denitrification rate of the Ce : Mn ratio of 5 : 1 reaching 58%. As the temperature continued to increase, the catalytic activity of the catalysts started to decrease and as this ratio showed a more excellent catalytic performance, a doping ratio of 5 : 1 Ce : Mn was determined as the optimum loading ratio.

3.1.2 Structural characteristics (XRD). Fig. 2 showed XRD patterns of different ratios of Mn loaded by the synthesis of $CeCO_3F$ plus natural monazite. From the figure, it can be observed that in all three catalysts loaded with different ratios of Mn, obvious diffraction peaks of cerium fluorocarbon can be observed and the intensity of the diffraction peaks is strong, which not only indicates a good synthesis effect, but also a good stability of the synthesised $CeCO_3F$ without decomposition after microwave roasting. From the figure, MnO_x species such as Mn_3O_4, Mn_2O_3 and MnO_2 can also be observed. Compared with the catalysts with Ce : Mn of 2 : 1 and 8 : 1, the diffraction peaks of MnO_x species on the 5 : 1 catalyst are relatively weak, which indicates that the dispersion of MnO_x species on the catalyst gradually becomes better and the Mn species are mainly dispersed on the catalyst surface in amorphous form,[14] not only that, there are more species of MnO_x species on its surface, and the interconversion between Mn ions is beneficial to improve the redox performance. As can be seen from the cell parameters in Table 1, the differences in grain size and crystalline spacing between the three are not significant. However, the catalyst with a Ce : Mn of 5 : 1 has a smaller spacing and size, indicating a relatively good dispersion of the carrier and active components, which is consistent with the activity test results. It was also observed that the diffraction peaks of cerium fluorocarbon also tended to fade and decrease compared to the other two catalysts, suggesting that the 5 : 1 catalyst was the best sample for the Mn loading.

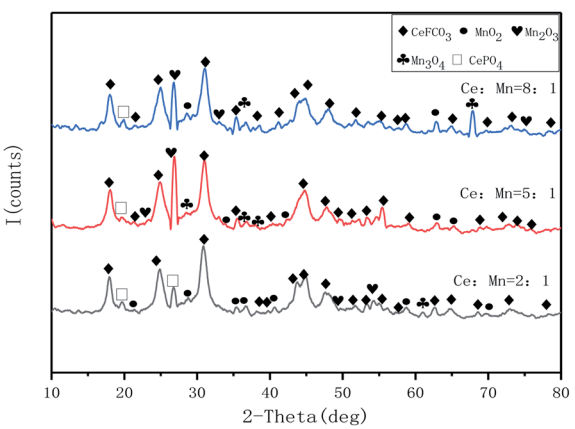

Fig. 2 XRD pattern of $CeCO_3F$-monazite loaded with different proportions of Mn.

Table 1 Physical structure properties of the catalysts

Catalysts	D (nm)	Crystallite dimension
Ce : Mn = 2 : 1	5.014	177
Ce : Mn = 5 : 1	5.142	147
Ce : Mn = 8 : 1	4.990	423

Table 2 The BET data of Samples

Samples	Surface area ($m^2\ g^{-1}$)	Pore volume ($ml\ g^{-1}$)	Pore size (nm)
Ce : Mn = 2 : 1	14.69	0.0109	10.10
Ce : Mn = 5 : 1	21.82	0.1252	35.36
Ce : Mn = 8 : 1	19.34	0.0963	35.30

3.1.3 Surface physical properties. The specific surface area test is one of the most important parameters to reflect the activity of the catalyst, it represents the contact area between the catalyst and the reaction medium in the catalytic reaction and directly affects the process of the catalytic reaction.

From Table 2, it can be seen that among the three catalysts with different loadings, the catalyst with a Ce : Mn ratio of 5 : 1 has a relatively large specific surface area, which provides more active sites for the NH_3-SCR reaction[15] and facilitates the adsorption of reactive gases on the catalyst surface.

3.2. The best active substances

3.2.1 Test of catalytic performance. The catalysts were loaded individually according to the optimum Mn and Fe loading ratios that had been determined, and then both were loaded simultaneously according to the same Mn and Fe ratios. As shown in Fig. 3.

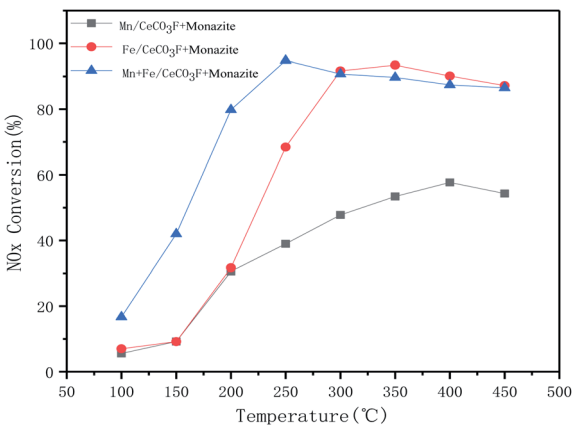

Fig. 3 NH_3-SCR activity of Mn and Fe loaded at the same time and NH_3-SCR activity of Optimum proportion of separate load Mn, Fe. (Reaction conditions: 500 ppm NO, 500 ppm NH_3, 3% O_2, N_2 as equilibrium gas)

The catalysts loaded with Fe alone showed very good activity in the range of 250 °C to 350 °C, up to 93%. This also indicated that the loading of Fe could better interact with the carrier to improve the catalytic activity. The catalysts loaded with both Mn and Fe reached 94.8% denitrification at 250 °C. Not only did they have good denitrification rates, but they also widened the temperature window and moved towards lower temperatures, with a decreasing trend in catalytic activity when the temperature exceeded 350 °C. This is due to the oxidation of ammonia gas, which can produce NO and NO_2 gas at higher temperatures.[16–18] The higher activity in the catalyst may lead to a rapid decrease in NO_x conversion at higher temperatures due to the increased redox capacity.[19] The increase in temperature provides energy that allows for enhanced interactions between Mn, Fe and Ce, thus facilitated conversion of NO and accelerated reduction of NO by NH_3. At higher temperatures, the movement and collisions of reacting molecules increase, so activity is enhanced in the low temperature range, however, the NH_3 oxidation side reaction (consumption of NH_3 reductant to produce N_2O, NO and NO_2) is the dominant reaction at higher temperatures, resulting in reduced catalytic activity.[18,20] Fig. 4 shows the stability of the catalytic activity of Mn + Fe/$CeCO_3F$ + monazite at 250 °C. It is clear that the catalyst can maintain the best denitrification effect at the appropriate temperature for a constant 15 h, which indicated that the denitrification performance is stable and not easily deactivated.

3.2.2 Structural characteristics (XRD). When loaded with Mn and Fe at the same time. As shown in the figure, only weak MnO_2 diffraction peaks were detected at 47.2°, 52.8° and 57.6°, which indicated that the Fe doping favoured a high degree of dispersion of the MnO_x species on the catalyst, while the intensity of the Fe oxide diffraction peaks was also very weak, which indicated a good dispersion of the Fe oxide species on the catalyst surface (Fig. 5).

In comparison with the catalyst loaded with Fe only, it can be clearly observed that the diffraction peak of Fe oxide is stronger than that of the catalyst loaded with both Mn and Fe, but the diffraction peak of cerium fluoride is significantly weaker than that of the catalyst loaded with Mn, which indicated that the doping of Fe can better promote the dispersion of the carrier, and the interaction between Fe and Ce is stronger than that

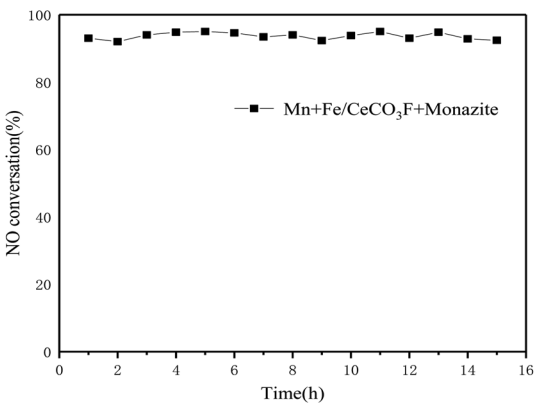

Fig. 4 Stability tests of the catalyst.

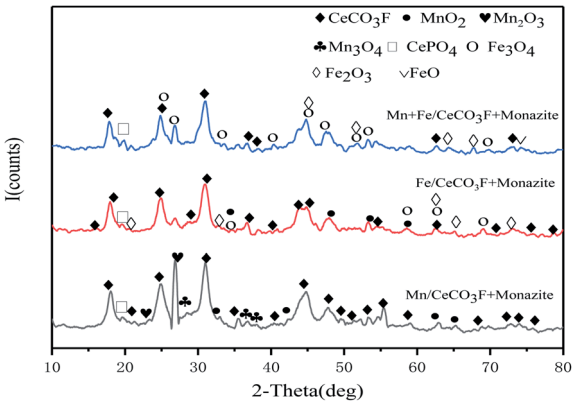

Fig. 5 XRD pattern of Mn and Fe loaded at the same time and Mn and Fe with separate loads.

between Mn and Ce. The catalysts loaded with Mn and Fe at the same time can have stronger interactions between the two, promoting each other's dispersion on the catalyst surface and thus improving the catalytic activity. From the cell parameters in Table 3, it can be seen that the composite catalysts loaded with both Mn and Fe have the largest grain surface spacing and a significant variation in grain size can be observed. Compared to the other catalysts, it has the smallest grain size, which also indicated that both manganese oxides and iron oxides were well loaded onto the catalyst surface.[21,23] This is further evidence of the good dispersion of the two, which fully exploits each other's catalytic activity and facilitates the NH_3-SCR reaction.

3.2.3 Surface physical properties. The enhanced pore capacity pore size in the BET data facilitates the diffusion of the reaction medium and the entry and exit of gases, which increase the reaction rate of the catalyst.[22] The very large specific surface area and pore size of the Fe-only loaded catalysts indicate that the Fe loading has better catalytic activity than the Mn loading alone, which is consistent with the XRD results. The specific surface area and pore volume pore size are the largest when loaded with both Mn and Fe, which can reach 28.92 $m^2 g^{-1}$. This indicates that Mn and Fe are well dispersed on the surface of the carrier, and their interaction can promote the dispersion of each other on the surface of the carrier, which is more conducive to the adsorption of reactive gases on the surface of the catalyst, and promote the SCR denitration reaction (Table 4).

3.2.4 Surface topography. Scanning electron microscopy was used to observe the surface structure of the catalyst. The graph showed that the catalyst with the optimum Mn loading had the active components distributed on the surface of the

Table 3 Physical structure properties of the catalysts

Catalysts	*D* (nm)	Crystallite dimension
Mn/$CeCO_3F$ + monazite	5.142	147
Fe/$CeCO_3F$ + monazite Mn	5.290	140
+ Fe/$CeCO_3F$ + monazite	5.833	131

Table 4 The BET data of Samples

Samples	Surface area ($m^2\ g^{-1}$)	Pore volume ($ml\ g^{-1}$)	Pore size (nm)
$Mn/CeCO_3F$ + monazite	21.82	0.1252	35.36
$Fe/CeCO_3F$ + monazite	27.16	0.1375	35.76
$Mn + Fe/CeCO_3F$ + monazite	28.92	0.1399	36.52

carrier in very fine particles and had a flat surface structure with slightly larger pores, which was consistent with the BET results. The catalyst loaded with Fe only has a better dispersion on the surface of the carrier, and the various types of material on the surface of the carrier are interspersed with each other, increasing the specific surface area. At the same time the catalyst loaded with Mn and Fe showed a large number of cracks on the surface, which may be due to the interaction of both Mn and Fe on the surface of the carrier, and prompt the conversion of large particles into smaller particles, which increased the number of active sites, these properties make this catalyst favourable to the adsorption and desorption behaviour of the gas. In addition, the microwave heating makes the surface of the particles show more cracks, and the characteristics of the microwave uniform heating makes the catalyst molecules oscillate, which increases the specific surface area of the catalyst and facilitates the improvement of denitrification efficiency (Fig. 6).

3.2.5 Reduction and desorption performance of catalyst. In order to investigate the low temperature redox capability of the

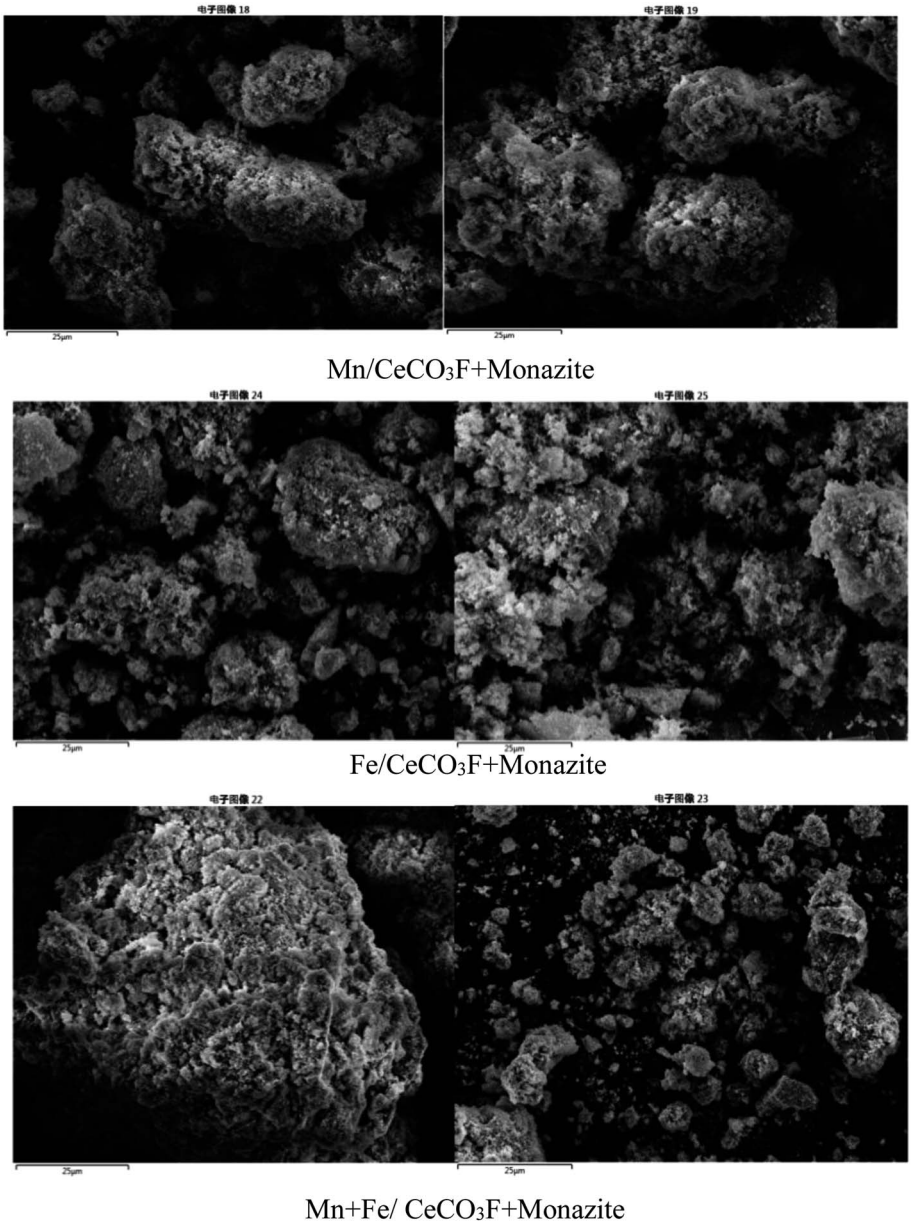

Fig. 6 SEM diagram of Mn and Fe loaded at the same time and Mn, Fe separate load.

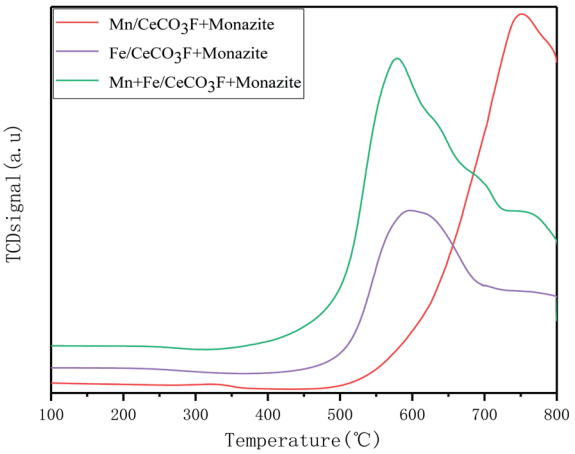

Fig. 7 H_2-TPR graph with Mn and Fe loaded at the same time and Mn and Fe loaded separately.

catalyst, it was characterised for H_2-TPR. It is well known that the redox properties of catalysts are a key factor in the oxidation of NO to NO_2 and can facilitate the fast SCR reaction [$NO + NO_2 + 2NH_3 \rightarrow 2N_2 + 3H_2O$] (Fig. 7).[23]

Stronger redox properties not only increase the oxidation rate of NO to NO_2 conversion but also improve the oxidation reaction activity. As can be seen from the figure, for the catalyst loaded with Mn has a higher H_2 reduction peak between 450 °C and 780 °C, which can be attributed to the process of MnO_2/$Mn_2O_3 \rightarrow Mn_3O_4 \rightarrow Mn$.[24–26] Due to the large variety of MnO_x species, the reaction process can be interconverted, which facilitates the redox reaction.[27] The reduction peaks in the high temperature section of the catalyst loaded with Mn at 700–780 °C, as obtained from the literature, can also be attributed to the reduction of the catalyst bulk phase CeO_2.[22,28] The catalysts loaded with both Fe and Mn showed reduction peaks at 575 °C, 690 °C and 760 °C, respectively, with the reduction peak at 575 °C attributed to the superposition of the reduction of Mn_3O_4 to MnO and the reduction of surface Ce^{4+} to Ce^{3+}.[22] The reduction peak at 690 °C can be attributed to FeO → Fe.[29] And when loaded with Fe and Mn at the same time, the position of the reduction peak moved towards the lower temperature compared to the other two catalysts. From Table 5 it can be seen that the area of their reduction peaks is the largest. This is probably due to the increase in reduction potential of the active component, the formation of oxygen vacancies and the appearance of more oxygen species on the surface, which facilitates the migration of oxygen and thus enhances the activation reaction of the catalysts, which indicated that the loading of Mn and Fe has greatly improved the redox properties of the catalysts. For the catalyst loaded with Fe only, a reduction peak appeared at 588 °C, which was attributed to the conversion of $Fe^{3+} \rightarrow Fe^{2+}$,[30] and the position of the reduction peak was at a lower temperature compared to the other catalysts, making it easier for the redox reaction to take place, but slightly less redox-friendly than the catalysts loaded with both Mn and Fe.

In addition to the redox properties, another key factor in NO removal is the adsorption and activation of NH_3 on the NH_3-SCR catalyst.[31] The desorption peaks in the TPD curves correspond to the surface acidic sites of the catalysts. From the figure, it can be seen that when loaded with both Mn and Fe, this catalyst shows two strong desorption peaks at 164 °C and 275 °C, which correspond to the Brønsted acid site and the Lewis acid site, respectively. The peak areas were significantly larger than the other two, as shown in Table 6, which indicated that this catalyst had the highest amount of acid and reflected the fact that it had the most acid sites and stronger adsorption of NH_3 than the other catalysts, which indicated better denitrification activity in the low temperature range. The catalyst loaded with only Fe also has peaks at 185 °C attributed to the desorption of weakly acidic sites, and 280 °C attributed to the desorption of moderately acidic sites. It follows that the low temperature peaks on the catalyst surface are associated with NH_4^+ on the Brønsted acidic sites and the high temperature peaks are associated with NH_3 on the Lewis acidic sites (Fig. 8).

To explore the adsorption behaviour of NO_x on the catalyst surface, the catalyst was characterised for NO-TPD and the formation of surface NO_x species is an important step in the NH_3-SCR reaction (Fig. 9).

It has been reported in the literature that low temperature desorption peaks near 100 °C correspond to physical and weak chemisorption of NO. The desorption peaks near 300 °C correspond to the desorption of mono-ligand nitrate or nitrite,

Table 5 H_2-TPR Suction and desorption curve peak area

In varying proportions	Mn/$CeCO_3F$ + monazite	Fe/$CeCO_3F$ + monazite	Mn + Fe/$CeCO_3F$ + monazite
Onset temperature (T/°C)	476	445	348
Peak temperature (T/°C)	748	599	571
Peak area	3085.57	4924.24	7936.72

Table 6 NH_3-TPD Suction and desorption curve peak area

In varying proportions	Mn/$CeCO_3F$ + monazite	Fe/$CeCO_3F$ + monazite	Mn + Fe/$CeCO_3F$ + monazite
Peak temperature (T/°C)	180, 475	185, 280	164, 275
Peak area	76.90	63.94	112.32

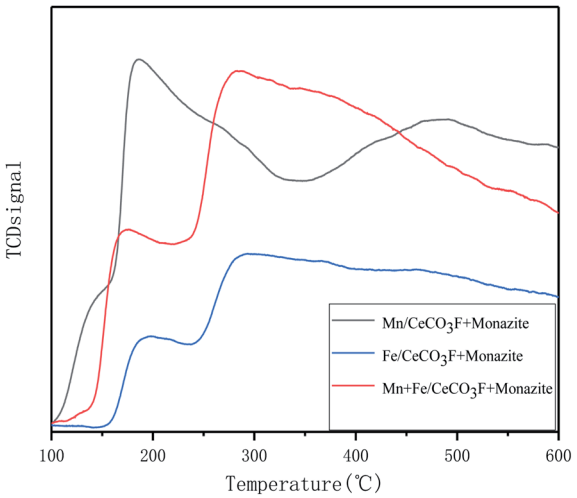

Fig. 8 NH_3-TPD graph with Mn and Fe loaded at the same time and Mn and Fe loaded separately.

and those above 300 °C correspond to the decomposition of double-ligand or bridged nitrate.[32–35] As can be seen from the figure, the catalyst loaded with Mn showed a desorption peak in the range of 100–250 °C. The NO-TPD reflects both the amount of NO adsorbed on the catalyst surface and the desorption temperature of NO on the catalyst surface, both of which can indirectly reflect the catalytic reactivity of the catalyst.[34,36] When Mn and Fe were loaded simultaneously, two very obvious desorption peaks appeared in the range of 100–500 °C. The area of the desorption peaks was the largest compared to the other two catalysts, and the location of the desorption peaks was also in the low temperature section, and the peak width and peak height also changed significantly. The effect was also changed, which indicated that the combined effect of Mn and Fe increased the adsorption capacity of the catalysts on NO, which resulted in a large amount of NO adsorption on the catalyst surface and increased the amount of acid and active sites on the catalyst surface. When only Fe was loaded, the area, peak position and intensity of the desorption peaks were similar to

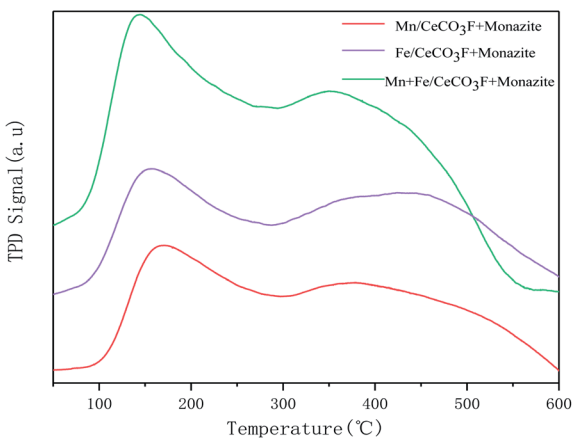

Fig. 9 NO-TPD graph with Mn and Fe loaded at the same time and Mn and Fe loaded separately.

Table 7 NO-TPD Suction and desorption curve peak area

In varying proportions	$Mn/CeCO_3F$ + monazite	$Fe/CeCO_3F$ + monazite	Mn + $Fe/CeCO_3F$ + monazite
Peak temperature (T/°C)	164, 389	153, 441	141, 358
Peak area	274.63	276.13	384.17

those of the Mn loading alone, which also indicated that there is no difference in the facilitation of NO adsorption by the catalyst between Mn and Fe loading alone, and when the two load together interact, they have a greater advantage to the catalyst for selective catalytic reduction of NO_x (Table 7).

3.3. *In situ* infrared analysis and reaction mechanism research

In order to investigated the types of adsorbed species on the catalyst surface and the role of each adsorbed species on the NH_3-SCR reaction, as well as its reaction mechanism under different temperature conditions, the Mn + $Fe/CeCO_3F$ + monazite composite catalysts were investigated *in situ* in the IR mechanism.

3.3.1 *In situ* infrared spectra of adsorption of NH_3 and NO + O_2 over time at 250 °C. In order to investigate the effect of the catalyst on the activation performance of NH_3 adsorption at low temperatures, this experiment investigated the variation of NH_3 adsorption with time at 250 °C, and the results are shown in Fig. 10. From the figure, it can be seen that the catalyst surface showed obvious infrared absorption peaks at 1109 cm^{-1}, 1192 cm^{-1}, 1293 cm^{-1}, 1698 cm^{-1} and 1826 cm^{-1}, where the absorption peaks at 1109 cm^{-1} were attributed to NH_4^+ species adsorbed on the Brønsted acidic site on the catalyst surface,[35] and the absorption peaks at 1192 cm^{-1}, 1293 cm^{-1}, 1698 cm^{-1} and 1593 cm^{-1} were attributed to NH_3 species adsorbed on the Lewis acidic site.[36,37] It can be seen that the predominant NH_3

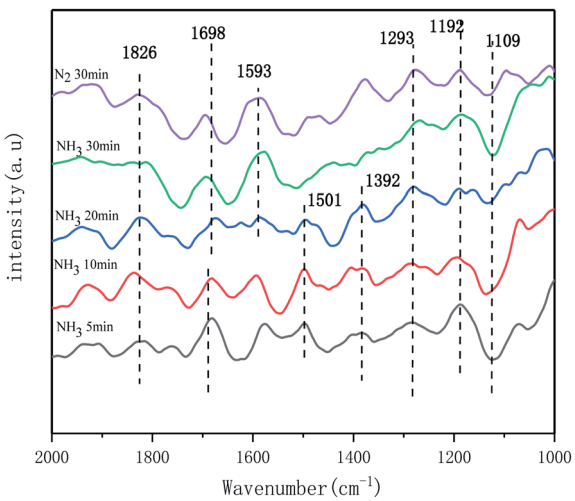

Fig. 10 *In situ* infrared spectra of NH_3 adsorbed by the catalyst at 250 °C.

adsorption site on the catalyst surface is the Lewis acidic site, with a small number of Brønsted acidic sites. Previous studies have shown that the presence of Brønsted acidic sites has a facilitative effect on the NH_3-SCR reaction.[38] The adsorption of the two acidic sites indicates that the acidic sites are abundant on the catalyst surface and that the NH_3 species and NH_4^+ species adsorbed on the catalyst surface are more stable with time.

The catalyst surface showed infrared absorption peaks at 1501 cm^{-1}, 1392 cm^{-1}, with the peak at 1392 cm^{-1} attributed to the deformation vibration of the N–H bond in the NH_4^+ adsorbed by the Brønsted acid centre on the catalyst surface,[39,41] and the absorption peak at 1501 cm^{-1} attributed to the amide ($-NH_2$) species, but the surface species gradually disappeared with increasing time, which indicated unstable adsorption.

To further investigated the effect of the catalyst on the NO adsorption and activation performance, the *in situ* IR spectra of NO + O_2 adsorption over time at 250 °C were also examined. As shown in Fig. 11, the infrared absorption peaks at 1937 cm^{-1}, 1834 cm^{-1}, and 1818 cm^{-1} were attributed to the weak adsorption species of NO formed on the catalyst surface,[40] and the adsorption species did not change much with increasing time, which indicated that it was more stable. The IR peak at 1115 cm^{-1} was attributed to the even secondary nitrate species [$-(N_2O_2)^{2-}$], the peak at 1211 cm^{-1} to the bridged nitrate species and 1310 cm^{-1} to the bidentate nitrate species. And the adsorbed species did not decrease with increasing time and N_2 purging. The peak at 1632 cm^{-1} was attributed to the weakly adsorbed NO_2 species on the catalyst surface. According to the literature,[40,42] NO_2 is an important intermediate species for the occurrence of fast SCR reactions under low temperature conditions. And the large number of adsorbed species on the catalyst surface indicates a very good activation capacity for NO adsorption.

3.3.2 *In situ* infrared spectra of NH_3 and NO + O_2 adsorbed species on the catalyst surface under different temperature conditions. In this experiment, the adsorption and activation of

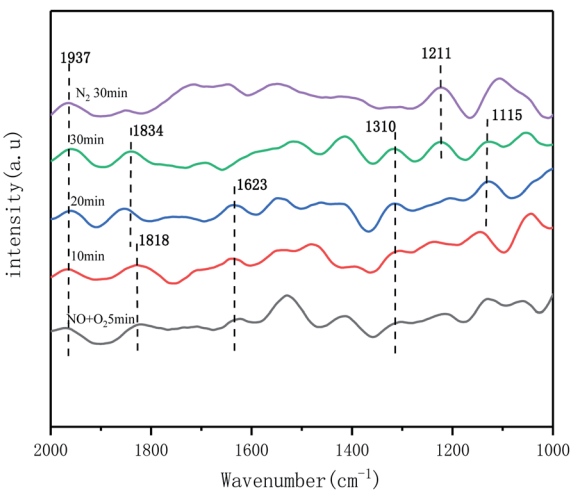

Fig. 11 NO + O_2 adsorption *in situ* infrared spectra of the catalyst at 250 °C.

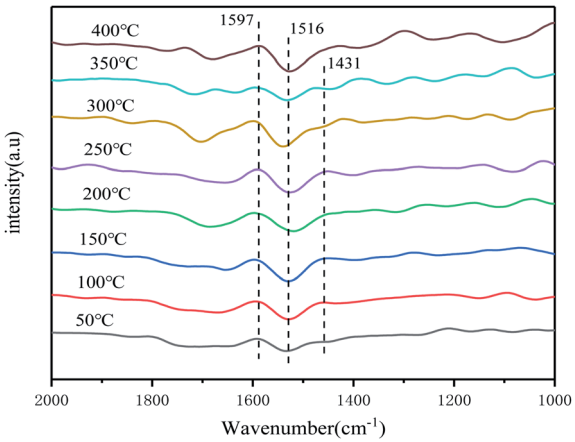

Fig. 12 *In situ* infrared spectra of NH_3 adsorption by the catalyst at different temperatures.

NH_3 on the catalyst surface at different temperatures was investigated by *in situ* IR spectroscopy, and the presence of NH_3 species on the catalyst surface at different temperatures was studied. As shown in Fig. 12, it is evident that the catalyst is present on the surface mainly in the form of NH_3 and NH_4^+. The catalyst shows infrared absorption peaks at 1431 cm^{-1}, 1516 cm^{-1} and 1597 cm^{-1}, where the absorption peak at 1431 cm^{-1} is attributed to NH_4^+ species adsorbed on the Brønsted acidic site on the catalyst surface,[37] and the absorption peak at 1516 cm^{-1} is attributed to the splitting of the bidentate nitrate due to the adsorption of NH_3 species by oxygen oxidation on the catalyst surface.[41] The absorption peak at 1597 cm^{-1} is attributed to liganded NH_3 species adsorbed on the Lewis acidic site on the catalyst surface. This shows that the main adsorption and activation sites for NH_3 species on the catalyst surface are the Brønsted acid site and the Lewis acid site. As the temperature increases, the absorption peak at 1431 cm^{-1} gradually decreases and almost disappears at 250 °C, indicated that the NH_4^+ species adsorbed on the Brønsted acid site on the catalyst surface are unstable and prone to thermal decomposition and desorption. However, the IR absorption peak at 1597 cm^{-1} did not change significantly with increasing temperature, which indicated that the NH_3 species adsorbed on the Lewis acid site on the catalyst surface were more stable, and only the NH_3 species on the Lewis acid site could be detected in the high temperature section, which suggested that the adsorption of NH_3 by the catalyst in the high temperature section was mainly carried out on the Lewis acid site.

The adsorption and activation processes of NO + O_2 species on the catalyst surface under different temperature conditions were subsequently investigated by *in situ* infrared spectroscopy, to discuss the forms and changes of NO_x species present on the catalyst surface under different temperature conditions. From Fig. 13, it can be seen that IR absorption peaks appeared on the catalyst surface at 1407 cm^{-1}, 1499 cm^{-1} and 1536 cm^{-1}, where all three peaks can be attributed to monodentate nitrate species,[39,42] and the IR absorption peak at 1617 cm^{-1} was attributed to bridged nitrate species.[38] As the temperature

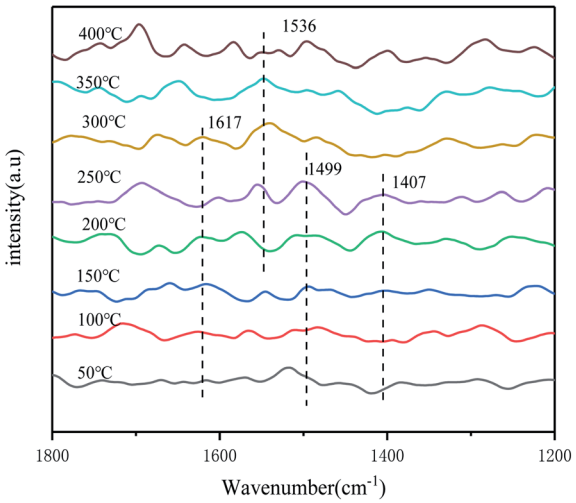

Fig. 13 *In situ* infrared spectra of NO + O_2 adsorption by the catalyst at different temperatures.

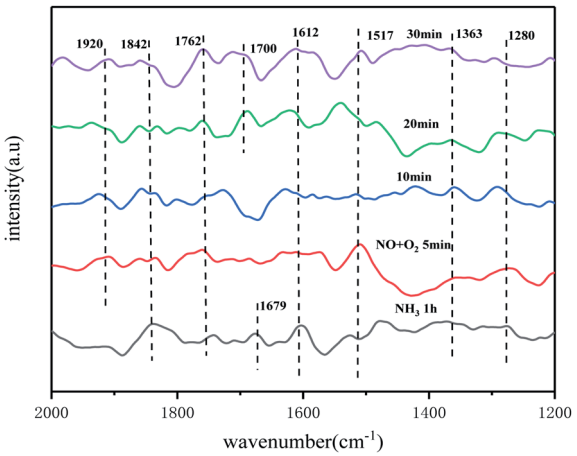

Fig. 14 *In situ* infrared spectra of NO + O_2 reacting with preadsorbed NH_3 species on the catalyst surface at 250 °C.

increased, the peaks of monodentate nitrate species at 1407 cm^{-1}, 1499 cm^{-1}, and bridged nitrate at 1617 cm^{-1} gradually decreased, which indicated that the adsorbed species on the catalyst surface began to undergo desorption and pyrolysis reactions, and the main active sites in the low temperature section were occupied by bridged nitrate and some of the monodentate nitrate. However, the monodentate nitrate species at 1536 cm^{-1} is more stable in the high temperature stage, which indicated that it has good thermal stability and occupies the active sites in the high temperature section. Therefore, it can be inferred that the NH_3-SCR reaction on the catalyst surface may follow different reaction paths due to different reaction temperatures.

3.3.3 *In situ* infrared spectra of reaction of NH_3 and NO + O_2 pre-adsorbed species on the catalyst surface at 250 °C. To further investigate the NH_3-SCR reaction mechanism of the catalyst, *in situ* IR spectroscopy of the catalyst was carried out at 250 °C under different reaction conditions. Firstly, NH_3 gas was passed into the IR reaction cell containing the catalyst for 60 min, prior to which N_2 was used as a supplementary gas to pre-treat the catalyst at 200 °C for 30 min, then the NH_3 gas was stopped and purged with N_2 for 10 min, after which NO + O_2 gas was then passed into the reaction cell. The changes in the IR spectrum were observed as shown in Fig. 14. First, the adsorption peak due to gaseous NH_3 appears at 1762 cm^{-1} after the passage of $NH_3$1h.[39] The absorption peaks at 1517 cm^{-1} and 1363 cm^{-1} were attributed to the adsorption of the ammonia dehydrogenation product NH_3^+ at the Brønsted acidic site and to the deformation movement of the mid-N-H bond in NH_4^+.[39] The peaks at 1280 cm^{-1}, 1612 cm^{-1} and 1679 cm^{-1} belong to NH_3 species adsorbed at Lewis acidic sites.[39,43,44] The abundant acidic sites on the catalyst surface may have been provided by the dropwise addition of manganese nitrate solution in addition to the carrier itself. After a subsequent purge of N_2 for 10 min, followed by the passage of NO + O_2 atmosphere for 5 min it was observed that the peaks belonged to NH_3 species at 1679 cm^{-1} and NH_4^+ species at 1363 cm^{-1} decreased, which indicated that both the Brønsted acidic site and the Lewis acidic site played a role. As the NO + O_2 pass time increased, absorption peaks appeared on the catalyst surface for the monodentate nitrate species (1280 cm^{-1} and 1517 cm^{-1}), the bridged nitrate (1612 cm^{-1}), and the bidentate nitrate species (1700 cm^{-1}) produced at 20 min pass time. The peak at 1762 cm^{-1} was attributed to the telescopic motion of N=O. The presence of O_2 facilitated the conversion of NO. The peaks at 1920 cm^{-1} and 1842 cm^{-1} belong to NO species in the weakly adsorbed state on the catalyst surface.[39] The monodentate nitrate species at 1517 cm^{-1} disappears after 10 min and is less stable, while the intensity of the other NO_x peaks gradually increases, which also indicates that both adsorbed NH_3 and NH_4^+ species are involved in the low temperature SCR reaction and react with the NO_x species produced.

Fig. 15 showed an *in situ* IR spectrum of the reaction of NH_3 with pre-adsorbed NO + O_2 species at 250 °C. At 250 °C temperature, when NO + O_2 was introduced into the reaction cell system for 60 min, the appearance of distinct monodentate

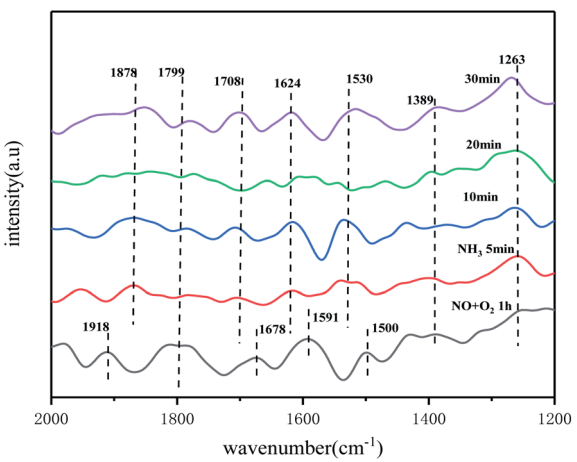

Fig. 15 *In situ* infrared spectra of NH_3 reacting with preadsorbed NO + O_2 species on the catalyst surface at 250 °C.

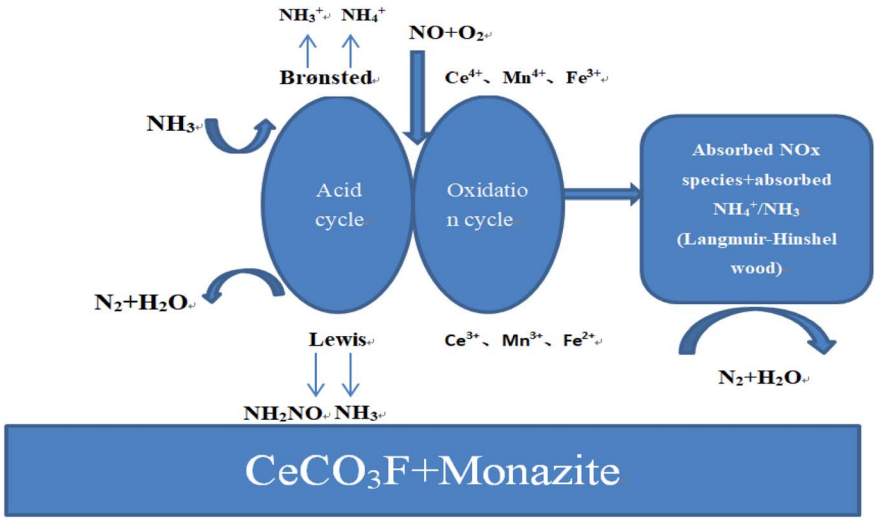

Fig. 16 L–H reaction mechanism of Mn + Fe/$CeCO_3F$-monazite.

nitrate species (1263 cm^{-1}, 1389 cm^{-1}, 1500 cm^{-1}),[45] bridged nitrate species (1591 cm^{-1}), and bidentate nitrate species (1678 cm^{-1}) can be observed on the catalyst surface. The IR absorption peak at 1799 cm^{-1} is attributed to the stretching motion of the N=O bond, and the peak at 1918 cm^{-1} is attributed to the weakly adsorbed species formed by NO on the catalyst surface. With the passage of NH_3, a significant weakening trend occurred for monodentate nitrate, bidentate nitrate and bridged nitrate species. The absorption peak disappeared at 10 min with increasing time of NH_3 introduction for all nitrate species. This also indicated that the nitrate species on the catalyst surface were partially involved in the reaction. With further passage of NH_3, NH_3 species adsorbed on the Lewis acidic site (1263 cm^{-1}) and NH_4^+ species adsorbed on the Brønsted acidic site appeared on the catalyst surface (1530 cm^{-1}, 1708 cm^{-1}).[35] The peaks at 1624 cm^{-1} and 1878 cm^{-1} belong to the active intermediate NH_2 after dehydrogenation of NH_3, while the peaks at 1799 cm^{-1} and 1389 cm^{-1} belong to the adsorption peak formed by gaseous NH_3 and the deformation vibration of the N–H bond in the NH_4^+ adsorbed at the Brønsted acid centre of the catalyst, respectively. The peak intensity is also more stable with increasing time, and some of the peaks show an enhancement trend. It can be concluded that the catalyst surface follows the L-H mechanism, where the nitrate species and NH_3/NH_4^+ species on the catalyst surface are the main intermediate species involved in the reaction, both of which undergo redox reactions on the catalyst surface to produce N_2 and H_2O. The catalytic mechanism is shown in Fig. 16.

4. Conclusion

In this experiment, $CeCO_3F$ was synthesised by hydrothermal method, and the synthesised $CeCO_3F$ was mixed with natural monazite ore as a carrier and loaded with Mn and Fe using the impregnation method. The optimum loading was determined by adding different ratios of amounts and the results showed that the best denitrification performance was achieved when Ce : Mn was 5 : 1. The load ratio is 1 : 1 for Fe : Mn, it was found that the composite catalyst supported by Fe and Mn at the same time showed excellent catalytic performance for denitrification, and the denitrification rate reached 94.8% at 250 °C. The loading of Mn and Fe played a very critical role in enhancing the catalytic activity, and their interaction promoted the dispersion of each other on the carrier surface, greatly increasing the specific surface area of the composite catalyst. Impregnation with manganese nitrate solution increased the acidic sites and the amount of acid. Microwave roasting resulted in the formation of more oxygen vacancies on the catalyst surface, which facilitated the migration of oxygen. *In situ* infrared spectroscopy was used to investigate the adsorption and activation properties of a new Mn–Fe/$CeCO_3F$-monazite catalyst for NO and NH_3 species, as well as the species and reaction behaviour of intermediate species in the NH_3-SCR reaction. The results showed that the NH_3-SCR reaction process occurring on the catalyst surface mainly follows the L–H mechanism. The bidentate nitrate and bridging nitrate species generated by the adsorption activation of gaseous NO on the catalyst surface and the NH_3/NH_4^+ species generated by NH_3 at the Lewis acidic site and Brønsted acidic site on the catalyst surface are the main intermediate species involved in the reaction, which undergo redox reactions to generate N_2 and H_2O on the catalyst surface. The excellent performance of $CeCO_3F$-monazite carriers provides a theoretical basis for the use of Baiyun Ebo rare earth minerals as denitrification catalyst carriers and high value utilization.

Conflicts of interest

There are no conflicts to declare.

Acknowledgements

This study was financially supported by Natural Science Foundation of Inner Mongolia (Grant No. 2019ZD13), National

Natural Science Foundation of China (Grant No. 51866013). Thanks for Start-up Funds for Talent Introduction and Scientific Research of Institutions in Inner Mongolia Autonomous Region.

References

1 F. Luck and J. Roiron, Selective catalytic reduction of NO_x emitted by nitric acid plants, *Catal. Today*, 1989, **4**(2), 205–218.

2 L. J. Alemany, F. Berti, G. Busca, G. Ramis, D. Robba, G. P. Toledo and M. Trombetta, Characterization and composition of commercial V_2O_5-WO_3-TiO_2 SCR catalyst, *Appl. Catal., B*, 1996, **10**(4), 299–311.

3 K. J. Lee, P. A. Kumar, M. S. Maqbool, K. N. Rao, K. H. Song and H. P. Ha, Ceria added Sb-V_2O_5/TiO_2 catalysts for low temperature NH_3-SCR: Physico-chemical properties and catalytic activity, *Appl. Catal., B*, 2013, **142–143**, 705–717.

4 F. D. Liu, H. He, C. B. Zhang, W. P. Shan and X. Y. Shi, Mechanism of the selective catalytic reduction of NO_x with NH_3 over environmental-friendly iron titanate catalyst, *Catal. Today*, 2011, **175**(1), 18–25.

5 J. P. Wang, Z. Yan, L. L. Liu, Y. Y. Zhang, Z. T. Zhang and X. D. Wang, Low-temperature SCR of NO with NH_3 over activated semi-coke composite-supported rare earth oxides, *Appl. Surf. Sci.*, 2014, **309**, 1–10.

6 J. Fan, P. Ning, Y. C. Wang, Z. X. Song, X. Liu, H. M. Wang, J. Wang, L. Y. Wang and Q. L. Zhang, Significant promoting effect of Ce or La on the hydrothermal stability of Cu-SAPO-34 catalyst fo NH_3-SCR reaction, *Chem. Eng. J.*, 2019, **369**, 908–919.

7 Z. L. Meng, B. W. Li, J. Y. Fu, C. Zhu and W. F. Wu, Research on NH_3-SCR denitrification performance of Fe_2O_3 mineral catalytic materials supported by rare earth concentrates, *Chin. J. Bioprocess Eng.*, 2020, **08–19**, 1–10.

8 K. Zhang, J. H. Zhu, S. N. Zhang, N. Li, H. J. Luo, B. W. Li, Z. W. Zhao, G. Jinang and W. F. Wu, Influence of Impurity Dissolution on Surface Properties and NH_3-SCR Catalytic Activity of Rare Earth Concentrate, *Minerals*, 2019, **9**(4), 246.

9 J. Wang, Z. J. Gong, B. W. Li, G. D. Xu and W. F. Wu, Mineral analysis of rare earth tailings and the effect of microwave roasting on its catalytic denitrification performance, *Mater. Rev.*, 2020, **34**(16), 16072–16076.

10 Z. H. Zhu, Z. F. Yang and Q. W. Wang, Research on Process Mineralogy of Bayan Obo Rare Earth Concentrate, *Nonferrous Met.*, 2019, (006), 1–4.

11 R. D. Zhang, W. Yang, N. Luo, P. X. Li, Z. G. Lei and B. H. Chen, Low-temperature NH_3-SCR of NO by lanthanum manganite perovskites: Effect of A-/B-site substitution and TiO_2/CeO_2 support, *Appl. Catal., B*, 2014, **146**, 94–104.

12 X. J. Yao, T. T. Kong, L. Chen, S. M. Ding, F. M. Yang and L. Dong, Enhanced low-temperature NH_3 -SCR performance of MnO_x/CeO_2 catalysts by optimal solvent effect, *Appl. Surf. Sci.*, 2017, **420**(31), 407–415.

13 N. Li, S. H. Zhang, H. Li, J. J. Wang, K. Zhang and W. F. Wu, Study on the microstructure and denitration performance of synthesized $CeCO_3F$, *J. Chin. Rare Earth Soc.*, 2020, **38**(5), 610–616.

14 T. Boningari, P. R. Ettireddy, A. Somogyvari, Y. Liu, A. Vorontsov, C. A. McDonald and P. G. Smirniotis, Influence of elevated surface texture hydrated titania on Ce-doped Mn/TiO_2 catalysts for the low-temperature SCR of NO_x under oxygen-rich conditions, *J. Catal.*, 2015, **325**, 145–155.

15 P. J. Gong, J. L. Xie, D. Fang, F. He, F. X. Li and K. Qi, Enhancement of the NH_3 -SCR property of Ce-Zr-Ti by surface and structure modification with P, *Appl. Surf. Sci.*, 2020, 505.

16 H. F. Chen, Y. Xia, H. Huang, Y. P. Gan, X. Y. Tao, C. Liang, J. M. Luo, R. Y. Fang, J. Zhang, W. K. Zhang and X. S. Liu, Highly dispersed surface active species of Mn/Ce/TiW catalysts for high performance at low temperature NH_3-SCR, *Chem. Eng. J.*, 2017, **330**, 1195–1202.

17 G. Ramis, L. Yi, G. Busca, M. Turco, E. Kotur and R. J. Willey, Adsorption, Activation, and oxidation of ammonia over SCR catalysts, *J. Catal.*, 1995, **157**(2), 523–535.

18 R. D. Zhang, W. Yang, N. Luo, P. X. Li, Z. G. Lei and B. H. Chen, Low-temperature NH_3-SCR of NO lanthanum manganite perovskites: effect of A-/B-site substitution and TiO_2/CeO_2 support, *Appl. Catal., B*, 2014, **146**, 94–104.

19 G. Y. Zhou, B. C. Zhong, W. H. Wang, X. J. Guan, B. C. Huang, D. Q. Ye and H. J. Wu, In situ DRIFTS study of NO reduction by NH_3 over Fe-Ce-Mn/ZSM-5 catalysts, *Catal. Today*, 2011, **175**, 157–163.

20 X. J. Yao, K. L. Ma, W. X. Zou, S. G. He, J. B. An, F. M. Yang and L. Dong, Influence of preparation methods on the physicochemical properties and catalytic performance of MnO_x-CeO_2 catalysts for NH_3-SCR at low temperature, *Chin. J. Catal.*, 2017, **38**(1), 146–159.

21 M. Xue. *Research on low-temperature SCR denitration performance and molding preparation of MnO_x-CeO_2 composite catalyst*, Northwest University, 2019.

22 N. L. Qiao, Y. X. Yang, Q. L. Liu, H. Q. Song, G. Z. Yu and M. S. Luo, The effect of the physical and chemical properties of the support on the denitration performance of manganese-cerium catalyst NH3-SCR, *J. Fuel Chem. Technol.*, 2018, **46**(06), 733–742.

23 E. Tronconi, I. Nova and C. Ciardelli, Redox features in the catalytic mechanism of the "standard" and "fast" NH_3-SCR of NO_x over a V-based catalyst investigated by dynamic methods, *J. Catal.*, 2007, **245**(1), 1–10.

24 Y. Xiong, C. J. Tang, X. J. Yao, L. Zhang, L. L. Li, X. B. Wang, Y. Deng, F. Gao and L. Dong, Effect of metal ions doping (M=Ti^{4+}, Sn^{4+}) on the catalytic performance of MnO_x/CeO_2 catalyst for low temperature selective catalytic reduction of NO with NH_3, *Appl. Catal., A*, 2015, **495**, 206–216.

25 X. F. Tang, Y. G. Li, X. M. Huang, Y. D. Xu, H. Q. Zhu, J. G. Wang and W. J. Shen, MnO_x-CeO_2 mixed oxide catalysts for complete oxidation of formaldehyde: Effect of preparation method and calcination temperature, *Appl. Catal., B*, 2006, **62**(3–4), 265–273.

26 Z. Wang, G. L. Shen, J. Q. Li, H. D. Liu, Q. Wang and Y. F. Chen, Catalytic removal of benzene over CeO_2-MnO_x

composite oxides prepared by hydrothermal method, *Appl. Catal., B*, 2013, **138–139**, 253–259.

27 B. Q. Jiang, *Preparation of Mn/TiO series low-temperature SCR denitrification catalyst and its reaction mechanism*, Zhejiang University, 2008.

28 D. Fang, J. Xie, H. Hu, H. Yang, F. He and Z. Fu, Identification of MnO x species and Mn valence states in MnO_x/TiO_2 catalysts for low temperature SCR, *Chem. Eng. J*, 2015, **271**, 23–30.

29 X. B. Huang, P. Wang, J. C. Tao and Z. S. Xi, CeO_2 modified Mn-Fe-O composite and its NH_3-SCR denitration catalytic performance, *J. Inorg. Mater.*, 2020, **35**(05), 573–580.

30 S. S. R. Putluru, L. Schill, A. D. Jensen, B. Siret, F. Tabaries and R. Fehrmann, Mn/TiO_2 and $Mn\text{-}Fe/TiO_2$ catalysts synthesized by deposition precipitation—promising for selective catalytic reduction of NO with NH_3 at low temperatures, *Appl. Catal., B*, 2015, **165**, 628–635.

31 C. J. Tang, L. Dong and H. L. Zhang, *Ceria-based catalysts for low-temperature selective catalytic reduction of NO with NH_3*, Catalysis science & technology, 2016.

32 F. D. Liu, H. He, Y. Ding and C. B. Zhang, Effect of manganese substitution on the structure and activity of iron titanate catalyst for the selective catalytic reduction of NO with NH_3, *Appl. Catal., B*, 2009, **93**(1), 194–204.

33 Z. H. Lian, F. Liu, H. He, X. Shi, J. Mo and Z. Wu, Manganese–niobium mixed oxide catalyst for the selective catalytic reduction of NO_x with NH_3 at low temperatures, *Chem. Eng. J.*, 2014, **250**(1), 390–398.

34 J. H. Zhu, *Study on the removal of impurities from rare earth concentrates and its NH_3-SCR denitration performance*, Inner Mongolia University of science and technology, 2019.

35 G. Ramis and M. A. Larrubia, An FT-IR study of the adsorption and oxidation of N-containing compounds over Fe_2O_3/AhO_3 SCR catalysts, *J. Mol. Catal. A: Chem.*, 2004, **215**(1–2), 161–167.

36 D. K. Sun, Q. Y. Liu, Z. Y. Liu, G. Q. Gui and Z. G. Huang, Adsorption and oxidation of NH_3 over V_2O_5/AC surface, *Appl. Catal., B*, 2009, **92**(3–4), 462–467.

37 L. Zhu, Z. P. Zhong, H. Yang, C. H. Wang and L. X. Wang, $DeNO_x$ performance and characteristic study for transition metals doped iron based catalysts, *Korean J. Chem. Eng.*, 2017, **34**(4), 1229–1237.

38 E. Borfecchia, K. A. Lomachenko, F. Giordanino, H. Falsig, P. Beato, A. V. Soldatov, S. Bordiga and C. Lamberti, Revisiting the nature of Cu sites in the activated Cu-SSZ-13 catalyst for SCR reaction, *Chem. Sci.*, 2015, **6**(1), 548–563.

39 Y. J. Liao, Y. P. Zhang, Y. X. Yu, J. Li, W. Q. Guo and X. L. Wang, In situ infrared study on the mechanism of $MnO_x/WO_3/TiO_2$ low temperature selective catalytic reduction of NO_x, *CIESC J.*, 2016, **67**(12), 5033–5037.

40 M. Bendrich, A. Scheuer, R. E. Hayes and M. Votsmeier, Unified mechanistic model for standard SCR, fast SCR, and NO_2 SCR over a copper chabazite catalyst, *Appl. Catal., B*, 2018, **222**, 76–87.

41 X. J. Yao, R. D. Zhao, L. Chen, J. Du, C. Y. Tao, F. M. Yang and L. Dong, Selective catalytic re-duction of NO_x by NH_3 over CeO_2 supported on TiO_2: Comparison of anatase, brookite, and rutile, *Appl. Catal., B*, 2017, **208**, 82–93.

42 L. L. Li, W. Tan, X. Q. Wei, Z. X. Fan, A. N. Liu, K. Guo, K. L. Ma, S. H. Yu, C. Y. Ge, C. J. Tang and L. Dong, Mo doping as an effective strategy to boost low temperature NH_3-SCR performance of CeO_2/TiO_2 catalysts, *Catal. Commun.*, 2018, **114**, 10–14.

43 Z. Liu, Y. Yi, J. Li, S. I. Woo, B. Wang, X. Cao and Z. Li, A superior catalyst with dual redox cycles for the selective reduction of NO_x by ammonia, *Chem. Commun.*, 2013, **49**, 7726–7728.

44 K. Liu, F. Liu, L. Xie, W. Shan and H. He, DRIFTS study of a Ce-W mixed oxide catalyst for the selective catalytic reduction of NO_x with NH_3, *Catal. Sci. Technol.*, 2015, **5**, 2290.

45 N. Z. Yang, R. T. Guo, Q. S. Wang, W. G. Pan, Q. L. Chen, C. Z. Lu and S. X. Wang, Deactivation of Mn/TiO_2 catalyst for NH_3-SCR reaction: effect of phosphorous, *RSC Adv.*, 2016, **6**(14), 11226–11232.